



UNIVERSITÀ POLITECNICA DELLE MARCHE  
Repository ISTITUZIONALE

Nanotechnology on wood: The effect of photocatalytic nanocoatings against *Aspergillus niger*

This is the peer reviewed version of the following article:

*Original*

Nanotechnology on wood: The effect of photocatalytic nanocoatings against *Aspergillus niger* / Goffredo, Giovanni Battista; Citterio, Barbara; Biavasco, Francesca; Stazi, Francesca; Barcelli, Sara; Munafò, Placido. - In: JOURNAL OF CULTURAL HERITAGE. - ISSN 1296-2074. - STAMPA. - 27:(2017), pp. 125-136. [10.1016/j.culher.2017.04.006]

*Availability:*

This version is available at: 11566/252305 since: 2022-05-25T11:43:03Z

*Publisher:*

*Published*

DOI:10.1016/j.culher.2017.04.006

*Terms of use:*

The terms and conditions for the reuse of this version of the manuscript are specified in the publishing policy. The use of copyrighted works requires the consent of the rights' holder (author or publisher). Works made available under a Creative Commons license or a Publisher's custom-made license can be used according to the terms and conditions contained therein. See editor's website for further information and terms and conditions.

This item was downloaded from IRIS Università Politecnica delle Marche (<https://iris.univpm.it>). When citing, please refer to the published version.

(Article begins on next page)

# **Nanotechnology on wood: The effect of photocatalytic nanocoatings against *Aspergillus niger***

Giovanni Battista Goffredo<sup>a</sup>, Barbara Citterio<sup>b</sup>, Francesca Biavasco<sup>c</sup>, Francesca Stazi<sup>d</sup>, Sara Barcelli e Placido Munafò<sup>a</sup>

<sup>a</sup> Department of civil and building engineering and architecture, polytechnic university of Marche, 12, via Brece Bianche, 60131 Ancona, Italy

<sup>b</sup> Department of biomolecular science, biotechnology section, university of Urbino “Carlo Bo”, 2, via Arco d’Augusto, 61032 Fano, Italy

<sup>c</sup> Department of life and environmental sciences, polytechnic university of Marche, 12, via Brece Bianche, 60131 Ancona, Italy

<sup>d</sup> Department of science and engineering of matter and environment and urban planning (SIMAU), polytechnic university of Marche, 12, via Brece Bianche, 60131 Ancona, Italy

<sup>e</sup> Department of pure and applied sciences, university of Urbino, 13, Piazza della Repubblica, 61029 Urbino, Italy

## Highlights

- Photocatalytic nanotreatments were used to protect wood from *Aspergillus niger*.
- Nanocoatings were aesthetically compatible with wooden artefacts.
- Antifungal efficiency was established combining different quantitative parameters.
- TiO<sub>2</sub>-based treatments partially restrained *A. niger* colonisation on wood surfaces.
- The presence of metal nanoparticles did not greatly improve antifungal efficiency.

## Abstract

Fungi play a primary role in wood decay, including building and historical surfaces. Over the last years, nanotechnology has been used to preserve different type of surfaces from biodeterioration caused by the development of biological contaminants. In this study, photocatalytic titanium dioxide (TiO<sub>2</sub>) based nanocompounds (also containing silver and copper) were brushed on wood surfaces to evaluate biocidal ability against the development of soft-rot fungus *Aspergillus niger*. Five different nanotreatments were applied on two types of wood (softwood and hardwood). Compatibility with wooden substrates has been assessed using colorimetry. Antifungal capability of metallic nanotreatments was quantitatively evaluated considering different parameters: microscopic observation, chromatic variation, reflectance change and mould extent. Even though photocatalytic nanotreatments inhibited *A. niger* development only partially, they seem to be a promising tool to reduce harmful mould development and to better preserve wooden artefacts.

## Keywords

Titanium dioxide, Nanometals, Wooden artefacts, *Aspergillus niger*, Wood preservation, Antifungal capability

## 1. Introduction

Wood is a material widely used all over the world for different purposes, including construction industry and works of art [1], [2], [3]. It is usually very sensitive to biological attacks [4], especially by fungi and insects: this biodegradation causes both aesthetical damages and deterioration of the internal structure. The fungal decay is generally due to an infection caused by few fungal spores and is characterized by several stages: an early colonization stage with slight changes in wood colour and texture, an intermediate stage with significant alteration in strength, texture and colour and an advanced stage with total disruption of the wood structure [5]. *Aspergillus niger* is a soft-rot fungus, responsible for cavity formation (soft-rot decay type I) and erosion (type II) [6] detected in archaeological wood especially from terrestrial environments [7]. *A. niger* growth is typically associated with high moisture levels and low light intensity, causing structural issues and health problems including allergies, respiratory symptoms and asthma especially during prolonged indoor exposure [8]. Moreover, biological decay of wooden artefacts and structures is a serious problem for Cultural Heritage involving considerable restoration efforts and cultural losses associated with the ruin of architectural legibility [9].

Over the last decades, several protective treatments have been used to defend wood against fungal development [10], [11]. Most of them are organic or metallic biocides: generally copper,

silver, boron and zinc. Unfortunately, many of these traditional preservatives and consolidants may be dangerous to the environment (for example in the case of leaching of metallic compounds) or be not fully compatible with wooden objects, especially in the field of Cultural Heritage [8], [11], [12].

Nanotechnology – i.e. the fields of science involved in the manipulation of matter within a size ranging from 1 to 100 nm usually able to generate new properties, phenomena and functions related to nanometric dimensions and structures – presents a remarkable potential to create a new generation of wood preservatives. Nanotechnology has been lately involved in different fields, including construction industry and Cultural Heritage, to obtain multifunctional nanosized materials. In particular, nanomaterials typically have very different characteristics from the original corresponding element and behave in distinct and unpredictable ways [13], [14].

During the last decade, nanomaterials – and metallic nanocompounds in particular – have been used to protect wooden artefacts and structures as surface treatments against biodegradation and weathering [13], [14], [15], [16], [17], [18], [19], [20]. Nanomaterials usually present better characteristics than their macroscopic counterparts used for wood preservation, mainly because of their reduced size and high specific surface area: a greater ability to penetrate uniformly in the wood [9], [19], [21], higher dispersion stability which can be further increased by the addition of a surfactant [19], improved biocidal performances, increased efficiency in the long term [8], enhanced compatibility with binders able to increase affinity with wood polymers [8], [11], [13], [15], [19], [22]. The analyses showed that the behaviour of nanotreatments is not homogeneous and depends on several factors, including the characteristics of wood substrates and fungal species used. Metallic nanoparticles – mainly copper, silver, zinc, boron – usually exhibited good performances against fungal decay by white-rot or brown-rot, on the other hand they could be less efficient in stopping mould growth [13], [15], [19], [20]. Anyway, both efficiency and compatibility with treated substrates may be enhanced by the use of new nanomaterials.

Titanium dioxide (TiO<sub>2</sub> or titania) is among the most successful nanomaterials and it has been used as self-cleaning and self-sterilising treatments over different surfaces in the building sector [23], [24], [25], [26], [27], [28] and more recently for the protection of Cultural Heritage [29], [30], [31], [32], [33], [34]. The biocidal potential of TiO<sub>2</sub> is related to its photoactivity under UV illumination [35], [36], [37], [38], [39], [40], [41], [42], [43] and its use as antibacterial and antifungal on wood surfaces is still under preliminary investigation [8], [9], [39]. However, the intensity of mould growth is usually rated by visual estimation by operators [8], [13], [15], [19], [44], a method that remains something subjective [43], [45].

## **2. Research aim**

The main aim of this work is to evaluate the ability of nanometric TiO<sub>2</sub> compounds in combination with metallic nanoparticles – silver (Ag) or copper (Cu) – applied on wood surface by brushing to preventively inhibit the ascomycete *Aspergillus niger* growth with particular reference to the preservation of Cultural Heritage. The damages performed by this ascomycete in historical and cultural handworks are important because of its spread in several environments [7]. A combination of instrumental analyses was used in order to better quantify mould growth and consequently the efficiency of biocidal treatments used on wood surfaces. Two different types of wood, pine and beech, commonly used in historical buildings and for other typical elements of Cultural Heritage have been coated with selected nanotreatments and then exposed to biological contamination. This investigation represents a preliminary analysis to establish compatibility and efficiency of TiO<sub>2</sub> nanoparticles used to prevent biodegradation of wood surfaces.

### 3. Materials and methods

#### 3.1. Wood specimens

Two different wood species were used in this work: pine (*Pinus sylvestris* L.) and beech (*Fagus sylvatica* L.), belonging respectively to softwood (gymnosperms) and hardwood (angiosperms). The selected wood species are typically used in the field of Cultural Heritage for both structural purposes in buildings and handworks [1], [46], [47], [48], [49], [50]. Test specimens were prepared from sapwood (dimensions:  $7 \times 20 \times 70$  mm<sup>3</sup>) free from both damages and defects; ten specimens were used per wood species for each treatment, including untreated control specimens. All specimens were pre-weighed, dried in ventilated oven (24 h, 103 °C) and then conditioned at temperature  $25 \pm 2$  °C and relative humidity  $77 \pm 3\%$  for a week prior to treatment [51].

#### 3.2. Nanocompounds

Titanium dioxide aqueous suspensions (sols) were prepared by sol-gel method with tetrapropyl orthotitanate (TPOT 97%, Sigma-Aldrich) as titania precursor. TPOT was added dropwise to a bihydrate oxalic acid (Carlo Erba 99.8%) water solution, obtaining a precipitate formed by amorphous – and barely photoactive – TiO<sub>2</sub>. The sols were later processed within an autoclave at 134 °C with a 2.5 °C/min heating rate for 30 minutes in order to produce TiO<sub>2</sub> nanocrystals (mainly in the anatase phase) and increase their photocatalytic ability. The characteristics of the so formed TiO<sub>2</sub> nanocrystals were analysed in previous studies by means of X-ray diffraction and dynamic light scattering: both anatase and rutile crystals were detected (original average crystal size: 4 nm), generally aggregated in clusters with dimensions ranging from 40 to 50 nm [34], [52], [53], [54]. The photocatalytic property of TiO<sub>2</sub> was already confirmed – even in the long-term – in self-cleaning, depollution and biocidal tests carried out previously [34], [52], [53], [54].

Five nanotreatments were produced also varying the compounds composition: a pure TiO<sub>2</sub> aqueous solution (named “nT”, TiO<sub>2</sub> amount: 1 wt%), two sols containing both TiO<sub>2</sub> and Ag nanoparticles (named “nTA1” and “nTA5”, additional Ag content: 1 mol% [0.60 wt%] and 5 mol% [3.15 wt%] respectively), two sols containing both TiO<sub>2</sub> and Cu nanoparticles (named “nTC1” and “nTC5”, additional Cu content: 1 wt% and 5 wt% respectively). Silver and copper were chosen in order to use their own disinfecting ability and to enhance the photocatalysis of TiO<sub>2</sub> [13], [19], [26], [55], [56], [57], [58], [59], [60], [61], [62]. Their concentrations were limited in order to avoid undesired colour changes (mostly browning) of the coatings on treated surfaces, as reported in literature [33], [34], [63], [64]. Nanotreatments used are listed and described in Table 1.

Table 1. Nanoproducts tested, designations – samples identified by a wood id-letter, nanotreatment acronym and a number standing for the percentage of metallic nanoadditives used in the sol composition – and amount of sol applied on wood (average values  $\pm$  standard deviation,  $n = 10$ ).

TABELLA

#### 3.3. Fungus and media used in the experiments

The strain of *Aspergillus niger* (F18) belongs to the Urbino university culture collection; it was revitalized on Potato Dextrose Agar (Oxoid) Petri dishes incubated for 5–7 days at  $28 \pm 0.5$  °C.

### 3.4. Methods

#### 3.4.1. Preparation and characterization of wood specimens

The nanoproducts were applied on wood brushing the upper surface of specimens. Ten specimens were used for each condition, including ten references. This method was preferred to vacuum treatment or dipping often used to apply protective nanoparticles on wood [8], [13], [14], [15], [16], [17], [19], [65], [66] since it is more similar to real treatments used on pre-existing wood surfaces. Average quantity of sol (total amount including the aqueous component estimated by weighing) deposited on treated specimens per nanoproduct and substrate are reported in Table 1.

The aesthetic compatibility between surface treatments and substrates is crucial for the preservation of Cultural Heritage. In order to assess visual compatibility with wood surfaces, colourimetric measurements were carried out before and after treatment with the aid of a Konica Minolta CM 2000 D portable spectrophotometer set up according to the CIE standards (observer angle: 10°, daylight illuminant: D65, measuring area diameter: 3 mm, wavelength range: 360–740 nm [67]). The results were expressed using the CIELAB colour model based on three chromatic coordinates: lightness  $L^*$  ranging from 0 (black) to 100 (white), the red/green parameter  $a^*$  (positive values towards red and negative ones towards green) and the yellow/blue parameter  $b^*$  (positive values towards yellow and negative ones towards blue). Colour variations due to the coatings were calculated as:

(1)

in which  $L^*_t$ ,  $a^*_t$  and  $b^*_t$  and  $L^*_{or}$ ,  $a^*_{or}$  and  $b^*_{or}$  are the mean colour coordinates per specimen respectively after and before the application of the coating. Chromatic alteration of each specimen was determined considering the average of three measurements per surface before and after treatment, then colour changes  $\Delta E^*$  due to each treatment were calculated as the average of the colour variations of ten specimens per case.

Before the beginning of mould test treated specimens were dried at room temperature for 24 h and then conditioned again for four weeks at temperature of  $25 \pm 2$  °C and relative humidity of  $77 \pm 3\%$ .

Wood specimens were exposed to UVA light (wavelength range: 350–400 nm, irradiance value on wood surfaces:  $3.75 \pm 0.25$  W/m<sup>2</sup>) for 24 h to activate the potential biocidal ability of TiO<sub>2</sub>. The characteristics of illumination were similar to analyses used to assess self-cleaning property of nanometric TiO<sub>2</sub> [54], [68], [69] and were suitable to activate its photogenerated properties [26], [55], [70]. The exposure to UVA light was performed exclusively before inoculation of *A. niger* to avoid any mutagenic effects of ultraviolet radiation or disturbance in fungal development, since fungi are very sensitive to UV illumination. After UVA illumination, wood specimens were conditioned again in the same environment previously described for 1 month to ensure standard initial conditions of wood before the inoculation of fungus.

Scanning electron microscopy (SEM) was performed to evaluate the structure and chemical composition of coated and uncoated wood surfaces after preconditioning and treatment phases. An environmental scanning electron microscope (Field Emission Gun Environmental Electron Scanning Microscope, FEG-ESEM, Quanta 200, FEI, The Netherlands) equipped with an X-ray microprobe of an Energy Dispersive Spectroscopy (EDS, EDAX, Mahwah, NJ, USA) was used. The samples were observed using 10 and 20 kV acceleration voltages and analysed at 20 kV with a lifetime of 50 s. Samples were examined in low vacuum with a chamber pressure set at 0.8 Torr.

#### 3.4.2. Mould test

Conidia were harvested after cultivation for 7 days at  $28 \pm 0.5$  °C stirring the culture with a sterile 0.85% NaCl (Sigma–Aldrich St. Louis, MO, USA) solution containing 0.05% Tween 80 (Sigma–Aldrich St. Louis, MO, USA) for 5 min. The conidia suspension was gently probed with a pipette tip and filtered to separate conidia from hyphal fragments. The transmittances of the conidia suspensions were adjusted using a BOECO Germany S-30 Spectrophotometer to provide a final test inoculum of about 106 conidia/mL ( $OD_{\lambda 530}$  0.1); 10 µL of conidia solution were placed in the middle of wood specimens described above. The choice to perform the inoculum using only the conidia was made to reproduce dynamics of contamination commonly found in nature that utilize conidia for dissemination. Following inoculation, the wood specimens were arranged in Petri dishes and incubated for 4 weeks at  $25 \pm 2$  °C and relative humidity of  $90.51 \pm 2.81\%$ . At the end of the test, the mould growth was evaluated by means of several quantitative parameters.

### **3.4.3. Biocidal action efficiency**

Five different parameters have been used to assess the biocidal efficiency of nanocoatings on wood specimens.

#### **3.4.3.1. Observation by stereomicroscope**

Firstly, after 2 weeks specimens were observed by a STEMI 508 (Zeiss) stereomicroscope to assess the conidia germination and mycelium development on wood.

Subsequently, after 4 weeks following the incubation, the intensity of mycelium development and of conidia formation was estimated by the following analyses.

#### **3.4.3.2. Observation by SEM**

To assess mycelium and conidia development and hyphae degradation using an environmental scanning electron microscope with 15 kV acceleration voltages.

#### **3.4.3.3. Colourimetry**

At the end of the mould test surface colour was measured through the same procedure used previously to determine colour changes before and after treatment, monitoring the same three points per specimen. Colour differences per specimen (referred to surface aspect post-treatment) due to the *A. niger* conidia development on wood were considered as the average of three monitored points, then colour changes per case were calculated as the mean of 10 specimen.

#### **3.4.3.4. Spectrophotometry**

The fungal development – depending on conidia formation – was also detected by spectrometry performed in conjunction with colour measurements before fungal inoculation and at the end of the mould test. Three measurement points were used per sample surface. The reflectance spectra of sample surfaces for visible light (390–740 nm) were measured to evaluate conidial heads colour [71], considering that the black appearance of *A. niger* conidial heads is probably due to the mixture of two pigments that compose the melanin: the green component (maximum absorption of light around 575 nm) and the brown one (absorbance peak at about 425 nm) [72]. The intensity of conidia development was defined as the average change of reflectance of surfaces at both specified wavelengths after 4 weeks of mould growth

due to melanin with reference to the original (OR) values preceding fungal inoculation:  
(2)

with R425,or and R425,4w being the percentage of light reflectance at a wavelength of 425 nm respectively before inoculation and after 4 weeks (end of mould test), R575,or and R575,4w the analogous percentages of light reflectance at 575 nm. The average of three measurement points used per surface determined the reflectance change for each specimen, the intensity of mould growth per analysed case was calculated consequently as the average of the corresponding ten specimens.

#### 3.4.3.5. Digital image analysis

Furthermore, the extent of area colonised by *A. niger* was assessed by means of digital image analysis (DIA) – similarly to procedures used for the estimation of biological growth on architectural surfaces [34], [37], [38], [43], [73], [74], [75], [76] – by ImageJ 1.48 v software. Specimens were scanned before inoculation and at the end of the mould test by a Canon CanoScan LiDE 700F with an image resolution of 600 dpi. The use of a scanner ensured the repeatability of test conditions: mainly observation angle, lightning, exposure and resolution. To establish the percentage of area contaminated by mould compared to total available surface, the K-means-like method was adopted, processing the images through a clustering procedure into a given number of classes, each one composed of a uniform colour zone. This algorithm separates chromatically similar pixels of the image (according to RGB colour model) into an arbitrary k number of groups selected by the operator, converting the original picture into a greyscale image by an automatic classification and assigning a specific grey level to each class. In this work, K-means method was used to part uncolonised areas from darkened areas covered by mycelium or conidiophore hyphae. Since fungal growth was clearly separated into mycelium and conidiophore hyphae, two different classes were used to define the areas colonised by *A. niger*. After a preliminary visual comparison between original and processed images, a total of four different classes ( $k = 4$ ) per image was chosen to include non-colonised (two grey levels for wood veins), partially-colonized (mycelium), completely-colonised areas (hyphae). At the end of each DIA, the processed image was compared with original picture in order to recognise the correspondence between K-means classes and colonisation intensity. The extent of each different phase of mould growth (hyphae and conidia) was expressed as the percentage ratio between the area occupied by the correspondent class and the total area of the specimen. The percentages were obtained counting the pixels belonging to each partition by means of a graphics software. Sample images are provided in Fig. 1.

Download : [Download high-res image \(471KB\)](#)Download : [Download full-size image](#)

Fig. 1. DIA: K-means like method, partition in four classes at the end of mould test. Final conditions of R and nT cases on pine and beech have been selected as reference. Clusters k1 and k2 identified clean surfaces (light and dark wood veins respectively), k3 mycelium and k4 conidia areas.

The combination of colorimetry, spectral analysis and K-means partition allows to objectively quantify the aesthetical alteration caused by mould growth on wood, unlike rating based on simple visual estimate by operators.

#### 3.4.4. Statistical analysis

Statistical analysis was performed using one-way analysis of variance (ANOVA) with P-value,  $P = 0.05$  using the Tukey's honest significant difference (HSD).



## 4. Results

### 4.1. Preparation and characterization of wood specimens

SEM analyses (Fig. 2, Fig. 3) revealed that the untreated wood surfaces (P\_R and B\_R) were characterised by several particles, different in size and nature (such as iron, calcium, silicates, barium sulphates, sodium chloride, gypsum and nickel) probably due to the cutting operations. Coatings on treated surfaces were rather uniform but differently affected by cracks wide up to 50  $\mu\text{m}$  (B\_nTA1, Fig. 3) probably due to the variable structure of wood (softwood or hardwood) and impurities present before treatment similarly detected on uncoated surfaces. The presence of cracked TiO<sub>2</sub>-containing nanocoatings has been detected already on several substrates and it is due mainly to excessive – and usually unnecessary – concentrations of TiO<sub>2</sub> used in the treatment or excessive quantities of the whole product deposited on treated surface [29], [31], [54]. Wooden surfaces treated only with TiO<sub>2</sub> presented different cracks: numerous, wide and parallel to the fibres on pine, smaller and with undefined principal direction on beech. Different cracks could be observed also in Ag-containing coatings: usually primary cracks developed parallel to fibres while secondary cracks were perpendicular (P\_nTA1 showed large primary cracks with very few secondary ones) with the exception of B\_nTA5 characterized by many cracks developed in all directions. The main cracks of Cu-containing coatings were parallel to the fibres, abundant and with different width; on beech secondary cracks had not a predominant direction. The presence of secondary cracks with no prevailing direction seemed to be more evident in Cu-containing coatings and generally on coatings applied to beech (Fig. 3).

The presence of titanium on all treated surfaces was confirmed clearly by EDX analyses of the coatings. In Ag-containing coatings (P\_nTA1, P\_nTA5, B\_nTA1, B\_nTA5) silver could be discerned in correspondence of areas rich in particles (Fig. 2, Fig. 3). The presence of Cu in the samples containing low percentages of it (P\_nTC1 and B\_nTC1) was not detected, instead – similarly to Ag-based treatments – its presence was clearly visible in rounded structures in P\_nTC5 and B\_nTC5 samples containing higher number of particles (Fig. 2, Fig. 3). The presence of other elements was related to pre-existing impurities already detected on untreated wood; this presence was less visible on treated surfaces since the uniformity of the coatings covered the impurities.

Chromatic variations due to treatment depended on both the characteristics of uncoated substrate and the composition of the nanoproducts. Table 2 shows colorimetric measurements before and after treatment. TiO<sub>2</sub> and Cu barely influenced the aspect of wood surfaces while Ag-containing coatings (namely nTA1 and nTA5) caused the most intense colour changes. Beech showed lower colour variations, with the highest values recorded again for Ag-treated surfaces. Higher concentrations of metallic nanoparticles did not necessarily cause higher chromatic variations.

### 4.2. Biocidal action efficiency

#### 4.2.1. Observation by stereomicroscope

Selected images from optical microscope – reported in Fig. 4 – show the capability of *A. niger* to colonize the wood 2 weeks following the conidia inoculation. The fungal colonization of untreated surfaces was quite homogenous and, from the central area of wood specimens, the mycelium spread all over the wood surface. Furthermore was clearly evident the presence of conidiophores aroused from the vegetative mycelium. On the contrary, fungal growth showed different behaviours on treated surfaces and was partially or totally inhibited: mycelium was

rarely detected, and conidia development was generally absent or limited to the inoculation area. It is interesting to note that on treated samples mycelium was more thin on coated site while on uncoated site (lateral borders), the hyphae appeared more thick and branched (Fig. 4). This difference between treated and untreated areas showed that under the same conditions the presence of biocidal nanotreatments is crucial to prevent fungal proliferation. Visual differences in the *A. niger* growth and conidia development were not observed in the two untreated wood species, although soft-rot is more common in hardwood than in softwood, because of the quality differences in the lignin of hard- and softwood. This could be attributed to the too short incubation time.

#### 4.2.2. Observation by SEM

SEM analysis performed at the end of the experiment (Fig. 5, Fig. 6) showed that, on treated surfaces, the reduced mycelium development matched with hyphal damage. It is well known that TiO<sub>2</sub> is a semiconductor photocatalyst, having an energy gap value ranging from 3.0 to 3.2 eV and capable of converting solar energy into chemical energy. Excitation of nano-TiO<sub>2</sub> by UV triggers oxidation processes and reactions, leading to the generation of Reactive oxygen species (ROS). Hydroxyl radicals ( $\bullet\text{OH}$ ), superoxide anion radicals ( $\bullet\text{O}_2^-$ ) and hydrogen peroxide (H<sub>2</sub>O<sub>2</sub>) are able to destroy bacteria, yeasts and moulds into CO<sub>2</sub> and H<sub>2</sub>O [79], [80], [81], [82], [83]. The process of TiO<sub>2</sub> photokilling starts with an oxidative attack to the polyunsaturated phospholipids, located in the microorganisms cell membrane [84]. Cell inability to counteract the structural and functional disorder of the inner membrane leads to death. That was evident in Fig. 5 where untreated pine surface showed cylindrical and swollen hyphae, whereas treated surfaces (Fig. 5B–D) showed hyphae not only less developed but also thinner, empty and fold (Fig. 5). The reduction of hyphal turgidity may be due to the damage of cell membrane that becomes unable to counteract the waste of solute, leading to the hyphal downfall. Also in beech (Fig. 6), it is possible to observe clear difference between untreated (Fig. 6A) and treated surfaces (Fig. 6B–D). The mycelium developed on untreated beech was plentiful and rich in conidia; on the other hand, on treated surfaces, the hyphae were sparser and showed the same damages seen on the pine (Fig. 6).

#### 4.2.3. Colourimetry

Colour changes measured at the end of the incubation time are reported in Fig. 7. Pine surfaces treated with the sole TiO<sub>2</sub> (nT) and the nanocompounds with the highest amount of metallic nanoparticles (nTA5 and nTC5) showed minor colour variations ( $\Delta E^*$  7.29, 6.95 and 7.05 respectively) compared to the control ( $\Delta E^*$  9.00), while the other treatments (nTA1 and nTC1) did not present any decrease ( $\Delta E^*$  9.11 and 9.38 respectively). On beech surfaces, only the treatments nT and nTA5 confirmed the behaviour showed in pine. The highest value of nTC5 ( $\Delta E^*$  6.50) was probably due to the irregular coating characterized by many cracks developed in all directions that allowed the fungus to reach the underlying untreated wood and to develop the conidia. In conclusion, after 4 weeks of incubation, in both wooden supports, pure TiO<sub>2</sub> coatings (nT) showed the best overall behaviour against conidia differentiation that do not seem to be influenced by the sterilising property of nanometallic particles added in the sols. The correlation of this result with the visual observation performed after 2 weeks reported above, showed as the TiO<sub>2</sub> not only reduced but also retarded the conidia development.

#### 4.2.4. Spectrophotometry

Reflectance spectra (Fig. 8) almost totally confirmed the results obtained by colorimetry.

Differences between cases were generally proportional to the differences in colour changes previously observed. In particular, pine surfaces P\_nT, P\_nTA5 and P\_nTC5 showed the best overall performance against conidia development causing a 20–30% decrease of mould intensity compared with untreated surfaces. The lowest value of reflectance reduction detected in P\_nTA5 (17.33%), not confirmed by colourimetry analysis, may be due to Ag-based treatments that applied on pine showed a visible colour variation ( $\Delta E^* = 7.53$ ) that could have affected the result. On beech only pure TiO<sub>2</sub> (B\_nT), and B\_nTA5 showed a restrained reduction (14.10% and 14.98% respectively) while the high value of the B\_nTC5 (20.51%) was due to the above reasoning (see Colourimetry). Treatments containing low amounts of metallic nanoadditives did not inhibit the mould development efficiently both in pine and in beech.

#### 4.2.5. Digital image analysis

The mould development determined by K-means method was arranged into two classes: mycelium and conidia. Differences between intermediate stereomicroscopy observation (2 weeks) and final digital image analysis (4 weeks) showed that mould growth and conidia differentiation were greater in the late part of the test. Results are summarised in Fig. 9. In pine, the area covered by mycelium growth, compared to the control (11.92%), showed a decrease in P\_nT, P\_nTC1 and P\_nTC5 (8.00%, 9.42% and 7.86% respectively), while the conidia were less present only in P\_nTC1 and P\_nTC5 (4.61% and 4.97% of wood surface occupied). Adding the values of mycelium and conidia, the most effective treatment was nTC5 (12.83%), confirming the efficacy of copper to inhibit *A. niger* development [85]. On beech, all the treatments were effective in countering mycelium growth, with best performances by B\_nT (7.89%) and B\_nTC5 (6.59%). Regarding the conidia development the efficiency of treatment nT (3.42%) was noticeable since the zone characterized by the presence of conidiophore hyphae was almost halved compared to control. The efficiency of treatment nT against mycelium growth was more homogeneous (the results showed the lowest standard deviations) and unrelated to infected substrate (about –35% of area extent in comparison with untreated surfaces for both wood species). Ag-containing treatments showed very limited effects and the mould development was comparable to the controls; furthermore, especially on pine, the conidia development was significant in comparison with the relative uncoated surfaces. On the contrary, the addition of Cu nanoparticles limited mould growth confirming a better efficacy of copper compared to silver to counteract *A. niger* development [85]. The results did not completely correspond to the outcomes of colorimetric and spectrophotometry analysis; particularly regarding silver (Ag) different results may be due to the higher colour changes originally induced in the wood.

#### 4.2.6. Statistical analysis

Statistical differences between biocidal efficiencies were quite limited. The only statistically relevant differences were noted for the area occupied by mould on beech treated with nT and nTC5 (statistical groups are shown exclusively in Fig. 9).

### 5. Discussion

The main aim of this work was to establish the efficiency of photocatalytic nanocoatings previously activated by UVA light against mould growth on wooden artefacts by the combination of different parameters based on colourimetry, spectral reflectance and image analysis, whereas usually visual observation is used in reference literature [8], [13], [15], [19],

[51]. Furthermore, the activation of photocatalytic treatments by UV light preceded the inoculation of fungus (without simultaneous presence) in order to avoid any interference between UV rays and fungal development and to better simulate the real conditions for the use of nanotreatments (activated only periodically and not uninterruptedly for preventive actions or during fungal growth). The inoculation using only conidia better reproduced the natural dynamics of contamination and allowed to discriminate the capability of the nanotreatments to inhibit both the conidia germination and their development. Furthermore, the inoculation in a single point and not on the whole specimen surface allowed to evaluate the capability of the fungus to spread from the site of infection and to colonize the surface.

Digital image analysis seems the more suitable evaluation technique since it is able to differentiate between area covered by the mycelium and the one covered by conidia. Nanocoatings caused a partial restriction of mould development, however the sole TiO<sub>2</sub> seems to be the main responsible for fungal inhibition since the presence of metallic nanoparticles did not necessary lead to an increase of biocidal efficiency, occasionally showing minor biocidal activity. This result could be due to the possible interaction between nanometals and the photocatalytic reaction, decreasing the ROS amount as well as the absorption of UV radiation by photocatalyst or the contact between the latter and the biological contaminant, consequently reducing the biocidal effectiveness of nanotreatments [86], [87], [88]. The biocidal effects of nanosilver compounds detected by other authors were obtained on different surfaces or at concentrations too high for their use on wooden surfaces typical of Cultural Heritage [85], [89]. Furthermore, the use of nanometals in combination with nanometric TiO<sub>2</sub> may reduce compatibility with selected substrates (higher chromatic changes due to treatment), increase the production costs and cause health problems related to the dispersion of metallic nanoparticles in the environment.

The performances of metal-containing sols depended on the amount of metallic nanoparticles used in the compounds: usually sols with higher percentage of metallic nanoparticles (nTA5, nTC5) were more efficient than their counterparts containing lesser amounts of the same metal (nTA1, nTC1 respectively) and did not alter the visual aspect of wooden surfaces significantly more.

This work represents a preliminary investigation since more research is needed on the factors that may influence the mould growth (e.g. humidity, temperature, inoculation) or, on the other hand, the efficiency of antifungal nanocoatings (such as nanoparticles type and dimensions, treatment procedure, intensity and duration of UV illumination). The limited statistical relevance could be due to the too short incubation time of mould development: indeed SEM images (Fig. 5, Fig. 6) showed hyphal degrade that in the long term could lead to more significant results. Moreover, different fungal species may cause different wood decay; so it is necessary to also test saprophytic fungi, like white and brown rot fungi, that attack the woody cell walls to better establish the effectiveness of antifungal treatments. Further studies are needed to better explore the mechanisms of biocidal action of nanoparticles and their performance conservation over time.

## 6. Conclusions

The outcome of the research is as follows:

- overall, nanocoatings were aesthetically compatible with wooden substrates, since the majority of colour changes measured after treatment could be considered acceptable even in the field of Cultural Heritage;
- nanotreatments previously activated by UVA illumination partially inhibited the growth of *A. niger*, especially the hyphal vitality and the extent of wood surfaces covered by fully germinated conidia;

- the metallic nanoparticles used to enhance the biocidal efficiency of TiO<sub>2</sub> did not bring evident benefits;
- digital image analysis was a better evaluation method compared to the visual analysis;
- further studies are required to establish the interactions between TiO<sub>2</sub> and metallic nanoparticles and their efficiency to inhibit fungal development on wood in a growth-friendly environment.

## Formatting of funding sources

This research did not receive any specific grant from funding agencies in the public, commercial, or not-for-profit sectors.

## Acknowledgements

We would like to thank the company Salentec srl (Lecce) for the kind supply of the nanoproducts used in this work. Professor Pietro Gobbi (University of Urbino) and Dr Claudio Pizzagalli (ARPAM Department, Pesaro) are highly acknowledged for the support provided for microscopic analyses.

## References

- [1]  
D. Hunt  
Properties of wood in the conservation of historical wooden artifacts  
J. Cult. Herit., 13 (2012), pp. S10-S15, 10.1016/j.culher.2012.03.014
- [2]  
P. Mazzanti, M. Togni, L. Uzielli  
Drying shrinkage and mechanical properties of poplar wood (*Populus alba* L.) across the grain  
J. Cult. Herit., 13 (2012), pp. S85-S89, 10.1016/j.culher.2012.03.015
- [3]  
B. Marcon, P. Mazzanti, L. Uzielli, L. Cocchi, D. Dureisseix, J. Gril  
Mechanical study of a support system for cupping control of panel paintings combining crossbars and springs  
J. Cult. Herit., 13 (2012), pp. S109-S117, 10.1016/j.culher.2012.04.003
- [4]  
C. Gaylarde, M. Ribas Silva, T. Warscheid  
Microbial impact on building materials: an overview  
Mater. Struct. Constr., 36 (2003), pp. 342-352, 10.1617/13867
- [5]  
P. Susi, G. Aktuganov, J. Himanen, T. Korpela  
Biological control of wood decay against fungal infection  
J. Environ. Manage., 92 (2011), pp. 1681-1689, 10.1016/j.jenvman.2011.03.004
- [6]

S.A.M. Hamed

In-vitro studies on wood degradation in soil by soft-rot fungi: *Aspergillus niger* and *Penicillium chrysogenum*

Int. Biodeterior. Biodegrad., 78 (2013), pp. 98-102, 10.1016/j.ibiod.2012.12.013

[7]

R.A. Blanchette

A review of microbial deterioration found in archaeological wood from different environments

Int. Biodeterior. Biodegrad., 46 (2000), pp. 189-204

[8]

F. Chen, X. Yang, Q. Wu

Antifungal capability of TiO<sub>2</sub> coated film on moist wood

Build. Environ., 44 (2009), pp. 1088-1093, 10.1016/j.buildenv.2008.07.018

[9]

G. De Filipo, A.M. Palermo, F. Rachiele, F.P. Nicoletta

Preventing fungal growth in wood by titanium dioxide nanoparticles

Int. Biodeterior. Biodegrad., 85 (2013), pp. 217-222, 10.1016/j.ibiod.2013.07.007

[10]

Alternative and conventional anti-fouling strategies

Int. Biodeterior. Biodegrad., 56 (2005), pp. 121-134, 10.1016/j.ibiod.2005.05.002

[11]

M. Shabir Mahr, T. Hübner, I. Stephan, H. Militz

Decay protection of wood against brown-rot fungi by titanium alkoxide impregnations

Int. Biodeterior. Biodegrad., 77 (2013), pp. 56-62, 10.1016/j.ibiod.2012.04.026

[12]

A. Unger

Decontamination and “deconsolidation” of historical wood preservatives and wood consolidants in cultural heritage

J. Cult. Herit., 13 (2012), pp. S196-S202, 10.1016/j.culher.2012.01.015

[13]

S.N. Kartal, F. Green, C.A. Clausen

Do the unique properties of nanometals affect leachability or efficacy against fungi and termites?

Int. Biodeterior. Biodegrad., 63 (2009), pp. 490-495, 10.1016/j.ibiod.2009.01.007

[14]

M. Bak, B.M. Yimmou, K. Csupor, R. Németh, L. Csóka

Enhancing the durability of wood against wood destroying fungi using nano-zinc

Int. Sci. Conf. Sustain. Dev. Ecol. Footpr. (2012)

[accessed February 3, 2015]

[https://bismarck.nyne.hu/fileadmin/dokumentumok/palyazat/tamop421b/IntConference/Papers/Articles/PDF/BakEtAl\\_EnhancingTheDurabilityOfWoodAgainstWoodDestroyingFungiUsingNanoZink.pdf](https://bismarck.nyne.hu/fileadmin/dokumentumok/palyazat/tamop421b/IntConference/Papers/Articles/PDF/BakEtAl_EnhancingTheDurabilityOfWoodAgainstWoodDestroyingFungiUsingNanoZink.pdf)

[15]

C.A. Clausen, V.W. Yang, R.A. Arango, F. Green III, F. Green III, R.A. Arango, S.T. Lebow

Feasibility of nanozinc oxide as a wood preservative

Proc Am Wood Prot. Assoc., 105 (2009), pp. 255-260

[16]

C.A. Clausen, F. Green, S. Nami, Kartal  
Weatherability and leach resistance of wood impregnated with nano-zinc oxide  
Nanoscale Res. Lett., 5 (2010), pp. 1464-1467, 10.1007/s11671-010-9662-6

[17]

C.A. Clausen, S.N. Kartal, R.A. Arango, F. Green III.  
The role of particle size of particulate nano-zinc oxide wood preservatives on termite mortality and leach resistance  
Nanoscale Res. Lett., 6 (2011), pp. 1-5

[18]

T. Künniger, A.C. Gerecke, A. Ulrich, A. Huch, R. Vonbank, M. Heeb, A. Wichser, R. Haag, P. Kunz, M. Faller  
Release and environmental impact of silver nanoparticles and conventional organic biocides from coated wooden façades  
Environ. Pollut., 184 (2014), pp. 464-471, 10.1016/j.envpol.2013.09.030

[19]

G. Mantanis, E. Terzi, S.N. Kartal, A.N. Papadopoulos  
Evaluation of mold, decay and termite resistance of pinewood treated with zinc- and copper-based nanocompounds  
Int. Biodeterior. Biodegrad., 90 (2014), pp. 140-144, 10.1016/j.ibiod.2014.02.010

[20]

C. Lykidis, M. Bak, G. Mantanis, R. Németh  
Biological resistance of pine wood treated with nano-sized zinc oxide and zinc borate against brown-rot fungi  
Eur. J. Wood Wood Prod., 74 (2016), pp. 909-911, 10.1007/s00107-016-1093-3

[21]

G.I. Mantanis, A.N. Papadopoulos  
The sorption of water vapour of wood treated with a nanotechnology compound  
Wood Sci. Technol., 44 (2010), pp. 515-522, 10.1007/s00226-010-0326-6

[22]

M.H. Freeman, C.R. McIntyre  
Copper-based wood preservatives  
For. Prod. J., 58 (2008), p. 7

[23]

W. Zhu, P.J.M. Bartos, A. Porro  
Application of nanotechnology in construction  
Mater. Struct., 37 (2004), pp. 649-658, 10.1617/14234

[24]

A. Fujishima, X. Zhang  
Titanium dioxide photocatalysis: present situation and future approaches  
Comptes Rendus Chim., 9 (2006), pp. 750-760, 10.1016/j.crci.2005.02.055

[25]

J. Chen, C. Poon  
Photocatalytic construction and building materials: from fundamentals to applications  
Build. Environ., 44 (2009), pp. 1899-1906, 10.1016/j.buildenv.2009.01.002

[26]

S. Guo, Z. Wu, W. Zhao

TiO<sub>2</sub>-based building materials: above and beyond traditional applications

Chin. Sci. Bull., 54 (2009), pp. 1137-1142, 10.1007/s11434-009-0063-0

[27]

F. Pacheco-Torgal, S. Jalali

Nanotechnology: advantages and drawbacks in the field of construction and building materials

Constr. Build. Mater., 25 (2011), pp. 582-590, 10.1016/j.conbuildmat.2010.07.009

[28]

K. Nakata, A. Fujishima

TiO<sub>2</sub> photocatalysis: design and applications

J. Photochem. Photobiol. C Photochem. Rev., 13 (2012), pp. 169-189,

10.1016/j.jphotochemrev.2012.06.001

[29]

A. Licciulli, A. Calia, M. Lettieri, D. Diso, M. Masieri, S. Franza, R. Amadelli, G. Casarano

Photocatalytic TiO<sub>2</sub> coatings on limestone

J. Sol-Gel Sci. Technol., 60 (2011), pp. 437-444, 10.1007/s10971-011-2574-9

[30]

L. Pinho, F. Elhaddad, D.S. Facio, M.J. Mosquera

A novel TiO<sub>2</sub>-SiO<sub>2</sub> nanocomposite converts a very friable stone into a self-cleaning building material

Appl. Surf. Sci., 275 (2013), pp. 389-396, 10.1016/j.apsusc.2012.10.142

[31]

E. Franzoni, A. Fregni, R. Gabrielli, G. Graziani, E. Sassoni

Compatibility of photocatalytic TiO<sub>2</sub>-based finishing for renders in architectural restoration: a preliminary study

Build. Environ., 80 (2014), pp. 125-135, 10.1016/j.buildenv.2014.05.027

[32]

P. Baglioni, E. Carretti, D. Chelazzi

Nanomaterials in art conservation

Nat. Nanotechnol., 10 (2015), pp. 287-290

[View PDFCrossRef](#)

[33]

P. Munafò, G.B. Goffredo, E. Quagliarini

TiO<sub>2</sub>-based nanocoatings for preserving architectural stone surfaces: an overview

Constr. Build. Mater., 84 (2015), pp. 201-218, 10.1016/j.conbuildmat.2015.02.083

[34]

G.B. Goffredo, S. Accoroni, C. Totti, T. Romagnoli, L. Valentini, P. Munafò

Titanium dioxide based nanotreatments to inhibit microalgal fouling on building stone surfaces

Build. Environ., 112 (2017), pp. 209-222, 10.1016/j.buildenv.2016.11.034

[35]

O.K. Dalrymple, E. Stefanakos, M.A. Trotz, D. Yogi, Goswami

A review of the mechanisms and modeling of photocatalytic disinfection

Appl. Catal. B Environ., 98 (2010), pp. 27-38, 10.1016/j.apcatb.2010.05.001

[36]

J. Hong, H. Ma, M. Otaki



Controlling algal growth in photo-dependent decolorant sludge by photocatalysis  
J. Biosci. Bioeng., 99 (2005), pp. 592-597, 10.1263/jbb.99.592

[37]

T. Martinez, A. Bertron, G. Escadeillas, E. Ringot  
Algal growth inhibition on cement mortar: efficiency of water repellent and photocatalytic treatments under UV/VIS illumination  
Int. Biodeterior. Biodegrad., 89 (2014), pp. 115-125, 10.1016/j.ibiod.2014.01.018

[38]

A. Maury-Ramirez, W. De Muynck, R. Stevens, K. Demeestere, N. De Belie  
Titanium dioxide based strategies to prevent algal fouling on cementitious materials  
Cem. Concr. Compos., 36 (2013), pp. 93-100, 10.1016/j.cemconcomp.2012.08.030

[39]

R. Oliva, A. Salvini, G. Di Giulio, L. Capozzoli, M. Fioravanti, C. Giordano, B. Perito  
TiO<sub>2</sub>-Oligoaldaramide nanocomposites as efficient core-shell systems for wood preservation  
J. Appl. Polym. Sci., 132 (2015), 10.1002/app.42047

[40]

J.R. Peller, R.L. Whitman, S. Griffith, P. Harris, C. Peller, J. Scalzitti  
TiO<sub>2</sub> as a photocatalyst for control of the aquatic invasive alga. *Cladophora*, under natural and artificial light  
J. Photochem. Photobiol. Chem., 186 (2007), pp. 212-217, 10.1016/j.jphotochem.2006.08.009

[41]

O. Seven, B. Dindar, S. Aydemir, D. Metin, M. Ozinel, S. Icli  
Solar photocatalytic disinfection of a group of bacteria and fungi aqueous suspensions with TiO<sub>2</sub>, ZnO and Sahara desert dust  
J. Photochem. Photobiol. Chem., 165 (2004), pp. 103-107, 10.1016/j.jphotochem.2004.03.005

[42]

C. Sichel, J. Tello, M. de Cara, P. Fernández-Ibáñez  
Effect of UV solar intensity and dose on the photocatalytic disinfection of bacteria and fungi  
Catal. Today., 129 (2007), pp. 152-160, 10.1016/j.cattod.2007.06.061

[43]

S.B. Vučetić, O.L. Rudić, S.L. Markov, O.J. Bera, A.M. Vidaković, A.S.S. Skapin, J.G. Ranogajec  
Antifungal efficiency assessment of the TiO<sub>2</sub> coating on façade paints  
Environ. Sci. Pollut. Res., 21 (2014), pp. 11228-11237, 10.1007/s11356-014-3066-6

[44]

M.F. La Russa, S.A. Ruffolo, N. Rovella, C.M. Belfiore, A.M. Palermo, M.T. Guzzi, G.M. Crisci  
Multifunctional TiO<sub>2</sub> coatings for cultural heritage  
Prog. Org. Coat., 74 (2012), pp. 186-191, 10.1016/j.porgcoat.2011.12.008

[45]

A. Fojutowski, A. Koziróg, A. Kropacz, A. Noskowiak  
The susceptibility of some acetylated hardwood species to mould fungi attack – An attempt to objectify the assessment  
Int. Biodeterior. Biodegrad., 86 (2014), pp. 60-65, 10.1016/j.ibiod.2013.08.007

[46]

I. Irbe, M. Karadelev, I. Andersone, B. Andersons  
Biodeterioration of external wooden structures of the Latvian cultural heritage

J. Cult. Herit., 13 (2012), pp. S79-S84, 10.1016/j.culher.2012.01.016

[47]

A. Jorissen

Structural interventions

J. Cult. Herit., 13 (2012), pp. S57-S63, 10.1016/j.culher.2012.05.001

[48]

M. Kisternaya, V. Kozlov

Preservation of historic monuments in the “Kizhi” Open-Air Museum (Russian Federation)

J. Cult. Herit., 13 (2012), pp. S74-S78, 10.1016/j.culher.2012.03.013

[49]

J.J. Łucejko, F. Modugno, M.P. Colombini, M. Zborowska

Archaeological wood from the Wieliczka Salt Mine Museum, Poland – Chemical analysis of wood degradation by Py(HMDS)-GC/MS

J. Cult. Herit., 13 (2012), pp. S50-S56, 10.1016/j.culher.2012.03.012

[50]

P. Palma, H. Garcia, J. Ferreira, J. Appleton, H. Cruz

Behaviour and repair of carpentry connections – rotational behaviour of the rafter and tie beam connection in timber roof structures

J. Cult. Herit., 13 (2012), pp. S64-S73, 10.1016/j.culher.2012.03.002

[51]

ASTM, D 4445-03 standard test method for fungicides for controlling sapstain and mold on unseasoned lumber (laboratory method), 2003.

[52]

E. Quagliarini, F. Bondioli, G.B. Goffredo, A. Licciulli, P. Munafò

Smart surfaces for architectural heritage: preliminary results about the application of TiO<sub>2</sub>-based coatings on travertine

J. Cult. Herit., 13 (2012), pp. 204-209, 10.1016/j.culher.2011.10.002

[53]

E. Quagliarini, F. Bondioli, G.B. Goffredo, A. Licciulli, P. Munafò

Self-cleaning materials on architectural heritage: compatibility of photo-induced hydrophilicity of TiO<sub>2</sub> coatings on stone surfaces

J. Cult. Herit., 14 (2013), pp. 1-7, 10.1016/j.culher.2012.02.006

[54]

P. Munafò, E. Quagliarini, G.B. Goffredo, F. Bondioli, A. Licciulli

Durability of nano-engineered TiO<sub>2</sub> self-cleaning treatments on limestone

Constr. Build. Mater., 65 (2014), pp. 218-231, 10.1016/j.conbuildmat.2014.04.112

[55]

K. Hashimoto, H. Irie, A. Fujishima

TiO<sub>2</sub> photocatalysis: a historical overview and future prospects

Jpn. J. Appl. Phys., 44 (2005), p. 8269, 10.1143/JJAP.44.8269

[56]

D.B. Hamal, J.A. Haggstrom, G.L. Marchin, M.A. Ikenberry, K. Hohn, K.J. Klabunde

A multifunctional biocide/sporicide and photocatalyst based on titanium dioxide (TiO<sub>2</sub>) codoped with silver, carbon, and sulfur

Langmuir, 26 (2010), pp. 2805-2810, 10.1021/la90.2844

[57]

M. Pelaez, N.T. Nolan, S.C. Pillai, M.K. Seery, P. Falaras, A.G. Kontos, P.S.M. Dunlop, J.W.J. Hamilton, J.A. Byrne, K. O'Shea, M.H. Entezari, D.D. Dionysiou

A review on the visible light active titanium dioxide photocatalysts for environmental applications

Appl. Catal. B Environ., 125 (2012), pp. 331-349, 10.1016/j.apcatb.2012.05.036

[58]

D. Pinna, B. Salvadori, M. Galeotti

Monitoring the performance of innovative and traditional biocides mixed with consolidants and water-repellents for the prevention of biological growth on stone

Sci. Total Environ., 423 (2012), pp. 132-141, 10.1016/j.scitotenv.2012.02.012

[59]

J.M. Coronado, F. Fresno, M.D. Hernández-Alonso, R. Portela (Eds.), Design of advanced photocatalytic materials for energy and environmental applications, Springer London, London (2013)

[60]

K. Naik, M. Kowshik

Anti-biofilm efficacy of low temperature processed AgCl-TiO<sub>2</sub> nanocomposite coating

Mater. Sci. Eng. C., 34 (2014), pp. 62-68, 10.1016/j.msec.2013.10.008

[61]

J. MacMullen, Z. Zhang, H.N. Dhakal, J. Radulovic, A. Karabela, G. Tozzi, S. Hannant, M.A. Alshehri, V. Buhé, C. Herodotou, M. Totomis, N. Bennett

Silver nanoparticulate enhanced aqueous silane/siloxane exterior facade emulsions and their efficacy against algae and cyanobacteria biofouling

Int. Biodeterior. Biodegrad., 93 (2014), pp. 54-62, 10.1016/j.ibiod.2014.05.009

[62]

E. Kowalska, Z. Wei, B. Karabiyik, A. Herissan, M. Janczarek, M. Endo, A. Markowska-Szczupak, H. Remita, B. Ohtani

Silver-modified titania with enhanced photocatalytic and antimicrobial properties under UV and visible light irradiation

Catal. Today., 252 (2015), pp. 136-142, 10.1016/j.cattod.2014.10.038

[63]

M.F. La Russa, A. Macchia, S.A. Ruffolo, F. De Leo, M. Barberio, P. Barone, G.M. Crisci, C. Urzì  
Testing the antibacterial activity of doped TiO<sub>2</sub> for preventing biodeterioration of cultural heritage building materials

Int. Biodeterior. Biodegrad., 96 (2014), pp. 87-96, 10.1016/j.ibiod.2014.10.002

[64]

S.A. Ruffolo, M. Ricca, A. Macchia, M.F. La, Russa

Antifouling coatings for underwater archaeological stone materials

Prog. Org. Coat., 104 (2017), pp. 64-71, 10.1016/j.porgcoat.2016.12.004

[65]

M. Schubert, T. Volkmer, C. Lehringer, F.W.M.R. Schwarze

Resistance of bioincised wood treated with wood preservatives to blue-stain and wood-decay fungi

Int. Biodeterior. Biodegrad., 65 (2011), pp. 108-115, 10.1016/j.ibiod.2010.10.003

[66]

D. Henriques, J. de Brito, S. Duarte, L. Nunes

Consolidating preservative-treated wood: combined mechanical performance of boron and polymeric products in wood degraded by *Coniophora puteana*

J. Cult. Herit., 15 (2014), pp. 10-17, 10.1016/j.culher.2012.11.008

[67]

UNI, UNI EN 15886 Conservation of cultural property Test methods Colour measurement of surfaces, 2010.

[68]

UNI, UNI 11259 Determinazione dell'attività fotocatalitica di leganti idraulici Metodo della rodammia, 2008.

[69]

B. Ruot, A. Plassais, F. Olive, L. Guillot, L. Bonafous

TiO<sub>2</sub>-containing cement pastes and mortars: measurements of the photocatalytic efficiency using a rhodamine B-based colourimetric test

Sol. Energy., 83 (2009), pp. 1794-1801, 10.1016/j.solener.2009.05.017

[70]

A. Fujishima, T.N. Rao, D. Tryk

TiO<sub>2</sub> photocatalysts and diamond electrodes

Electrochim. Acta., 45 (2000), pp. 4683-4690, 10.1016/S0013-4686(00)00620-4

[71]

J. Ważny, P. Rudniewski, K.J. Krajewski, T. Ważny

The reflectance method for testing the effectiveness of fungicides against surface mould growth on materials: I. Wood

Wood Sci. Technol., 23 (1989), pp. 179-189

[View PDF CrossRef](#)

[72]

T.R. Jørgensen, J. Park, M. Arentshorst, A.M. van Welzen, G. Lamers, P.A. van Kuyk, R.A.

Damveld, C.A.M. van den Hondel, K.F. Nielsen, J.C. Frisvad, A.F.J. Ram

The molecular and genetic basis of conidial pigmentation in *Aspergillus niger*

Fungal Genet. Biol., 48 (2011), pp. 544-553, 10.1016/j.fgb.2011.01.005

[73]

H. Barberousse, B. Ruot, C. Yéprémian, G. Boulon

An assessment of façade coatings against colonisation by aerial algae and cyanobacteria

Build. Environ., 42 (2007), pp. 2555-2561, 10.1016/j.buildenv.2006.07.031

[74]

W. De Muyck, A. Maury-Ramirez, N. De Belie, W. Verstraete

Evaluation of strategies to prevent algal fouling on white architectural and cellular concrete

Int. Biodeterior. Biodegrad., 63 (2009), pp. 679-689, 10.1016/j.ibiod.2009.04.007

[75]

G. Escadeillas, A. Bertron, E. Ringot, P.J. Blanc, A. Dubosc

Accelerated testing of biological stain growth on external concrete walls. Part 2: quantification of growths

Mater. Struct., 42 (2009), pp. 937-945, 10.1617/s11527-008-9433-3

[76]

Z. Zhang, J. MacMullen, H.N. Dhakal, J. Radulovic, C. Herodotou, M. Totomis, N. Bennett

Biofouling resistance of titanium dioxide and zinc oxide nanoparticulate silane/siloxane exterior facade treatments

Build. Environ., 59 (2013), pp. 47-55, 10.1016/j.buildenv.2012.08.006

[77]

C. Miliani, M.L. Velo-Simpson, G.W. Scherer

Particle-modified consolidants: a study on the effect of particles on sol-gel properties and consolidation effectiveness

J. Cult. Herit., 8 (2007), pp. 1-6, 10.1016/j.culher.2006.10.002

[78]

O. García, K. Malaga

Definition of the procedure to determine the suitability and durability of an anti-graffiti product for application on cultural heritage porous materials

J. Cult. Herit., 13 (2012), pp. 77-82, 10.1016/j.culher.2011.07.004

[79]

E.J. Wolfrum, J. Huang, D.M. Blake, P.-C. Maness, Z. Huang, J. Fiest, W.A. Jacoby

Photocatalytic oxidation of bacteria, bacterial and fungal spores, and model biofilm components to carbon dioxide on titanium dioxide-coated surfaces

Environ. Sci. Technol., 36 (2002), pp. 3412-3419, 10.1021/es011423j

[80]

K.P. Kühn, I.F. Chaberny, K. Massholder, M. Stickler, V.W. Benz, H.-G. Sonntag, L. Erdinger

Disinfection of surfaces by photocatalytic oxidation with titanium dioxide and UVA light

Chemosphere., 53 (2003), pp. 71-77, 10.1016/S0045-6535(03)00362-X

[81]

N. Akiba, I. Hayakawa, E.-S. Keh, A. Watanabe

Antifungal effects of a tissue conditioner coating agent with TiO<sub>2</sub> photocatalyst

J. Med. Dent. Sci., 52 (2005), pp. 223-227

[82]

D. Mitoraj, A. Jańczyk, M. Strus, H. Kisch, G. Stochel, P.B. Heczko, W. Macyk

Visible light inactivation of bacteria and fungi by modified titanium dioxide

Photochem. Photobiol. Sci., 6 (2007), pp. 642-648, 10.1039/B617043A

[83]

D. Pan, Z. Zhan, D. Chen, Z. Wu, A. Pang, Y. Wang, Z. Lin

Photocatalytic bactericidal mechanism of nanoscale TiO<sub>2</sub> films on Escherichia coli

J. Nanosci. Nanotechnol., 11 (2011), pp. 7621-7626, 10.1166/jnn.2011.4757

[84]

K. Sunada, T. Watanabe, K. Hashimoto

Studies on photokilling of bacteria on TiO<sub>2</sub> thin film

J. Photochem. Photobiol. Chem., 156 (2003), pp. 227-233, 10.1016/S1010-6030(02)00434-3

[85]

F.M. Helmi, N.M. Ali, S.M. Ismael

Nanomaterials for the inhibition of microbial growth on ancient egyptian funeral masks

Mediterr. Archaeol. Archaeom., 15 (2015), pp. 87-95

[86]

S. Ikeda, N. Sugiyama, B. Pal, G. Marcí, L. Palmisano, H. Noguchi, K. Uosaki, B. Ohtani

Photocatalytic activity of transition-metal-loaded titanium(IV) oxide powders suspended in

aqueous solutions: correlation with electron-hole recombination kinetics  
Phys. Chem. Chem. Phys., 3 (2001), pp. 267-273, 10.1039/b008028o

[87]

M. Anpo

The design and development of highly reactive titanium oxide photocatalysts operating under visible light irradiation

J. Catal., 216 (2003), pp. 505-516, 10.1016/S0021-9517(02)00104-5

[88]

R. van Grieken, J. Marugán, C. Sordo, P. Martínez, C. Pablos

Photocatalytic inactivation of bacteria in water using suspended and immobilized silver-TiO<sub>2</sub>

Appl. Catal. B Environ., 93 (2009), pp. 112-118, 10.1016/j.apcatb.2009.09.019

[89]

M.A. Shirakawa, C.C. Gaylarde, H.D. Sahrão, J.R.B. Lima

Inhibition of *Cladosporium* growth on gypsum panels treated with nanosilver particles

Int. Biodeterior. Biodegrad., 85 (2013), pp. 57-61, 10.1016/j.ibiod.2013.04.018

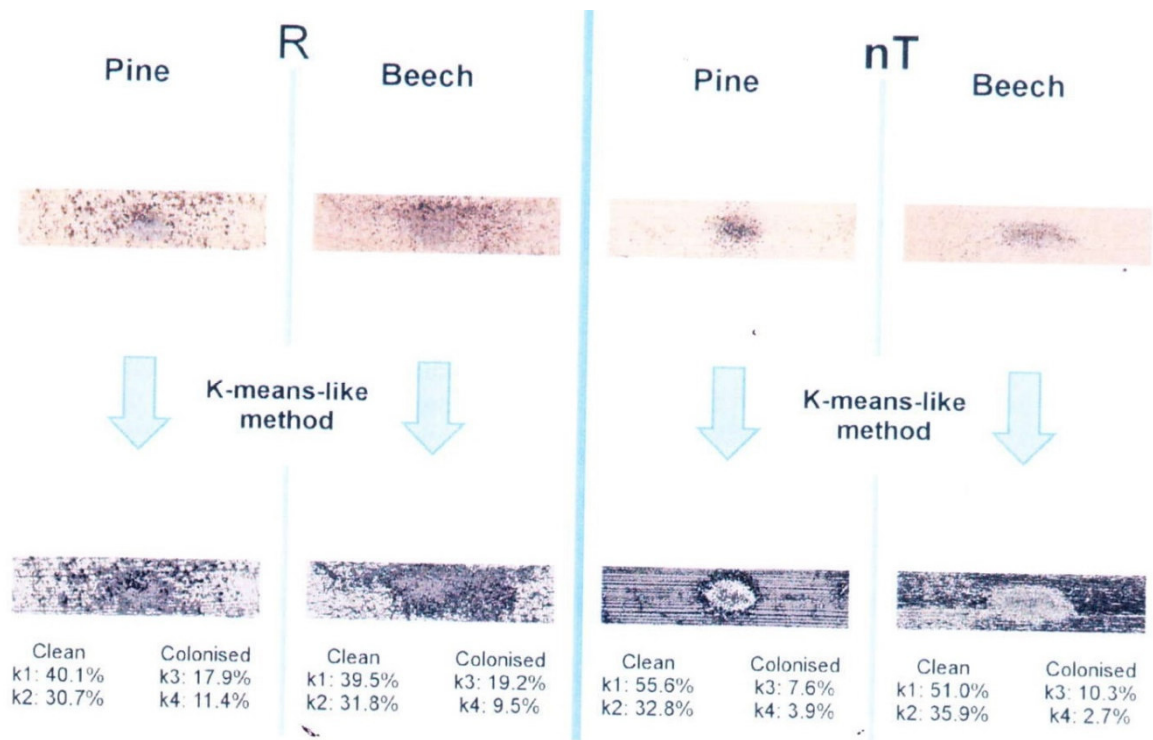


Fig. 1.DIA: K-means like method, partition in four classes at the end of mould test. Final conditions of R and nT cases on pine and beech have been selected as reference. Clusters k1 and k2 identified clean surfaces (light and dark wood veins respectively), k3 mycelium and k4 conidia areas.

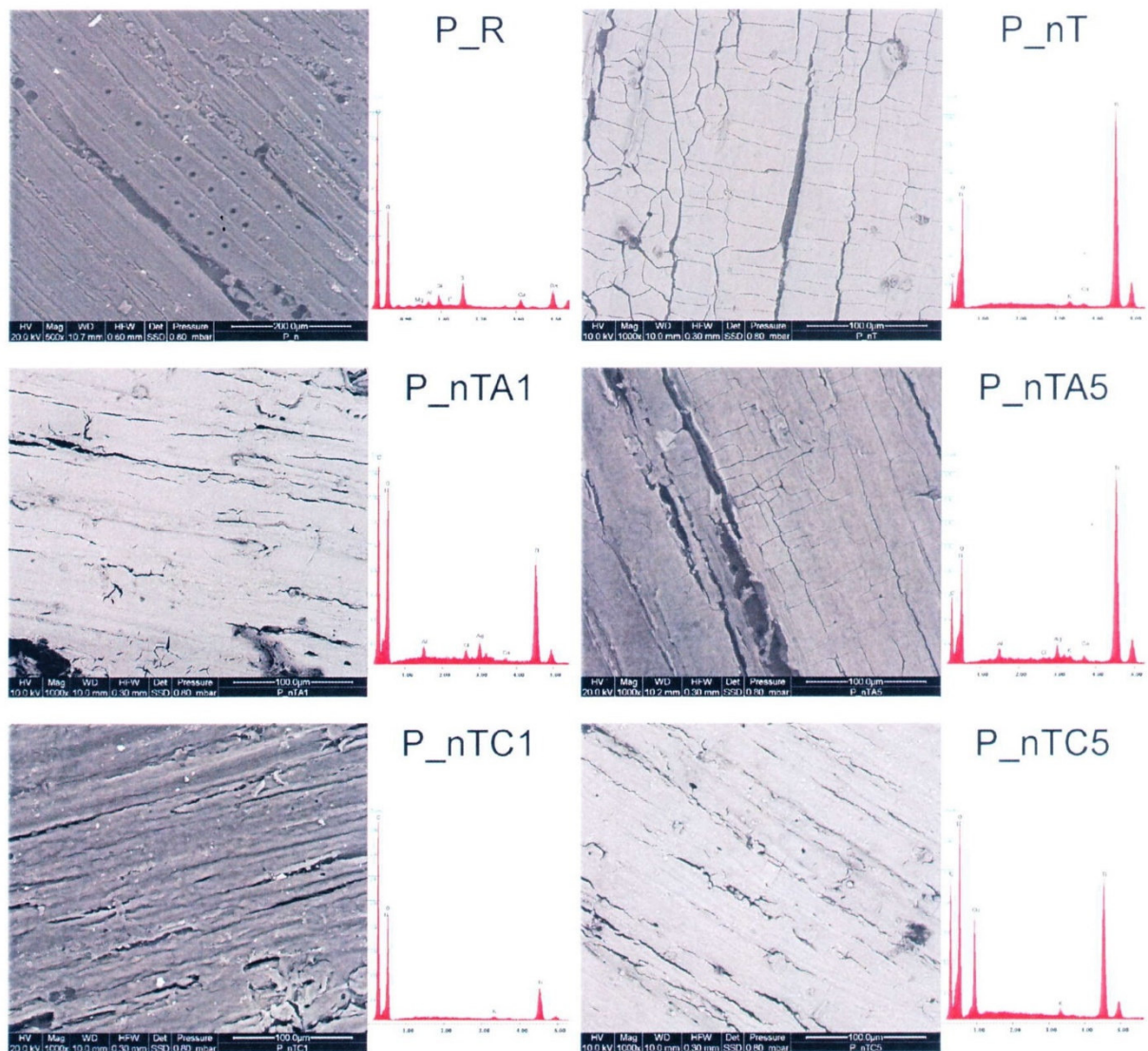


Fig. 2. Microscopic analyses of pine surfaces before mould test, untreated and treated: SEM images (magnitude 500× for untreated wood, 1.000× for treated surfaces) and EDS spectra (to the right of the corresponding SEM images)



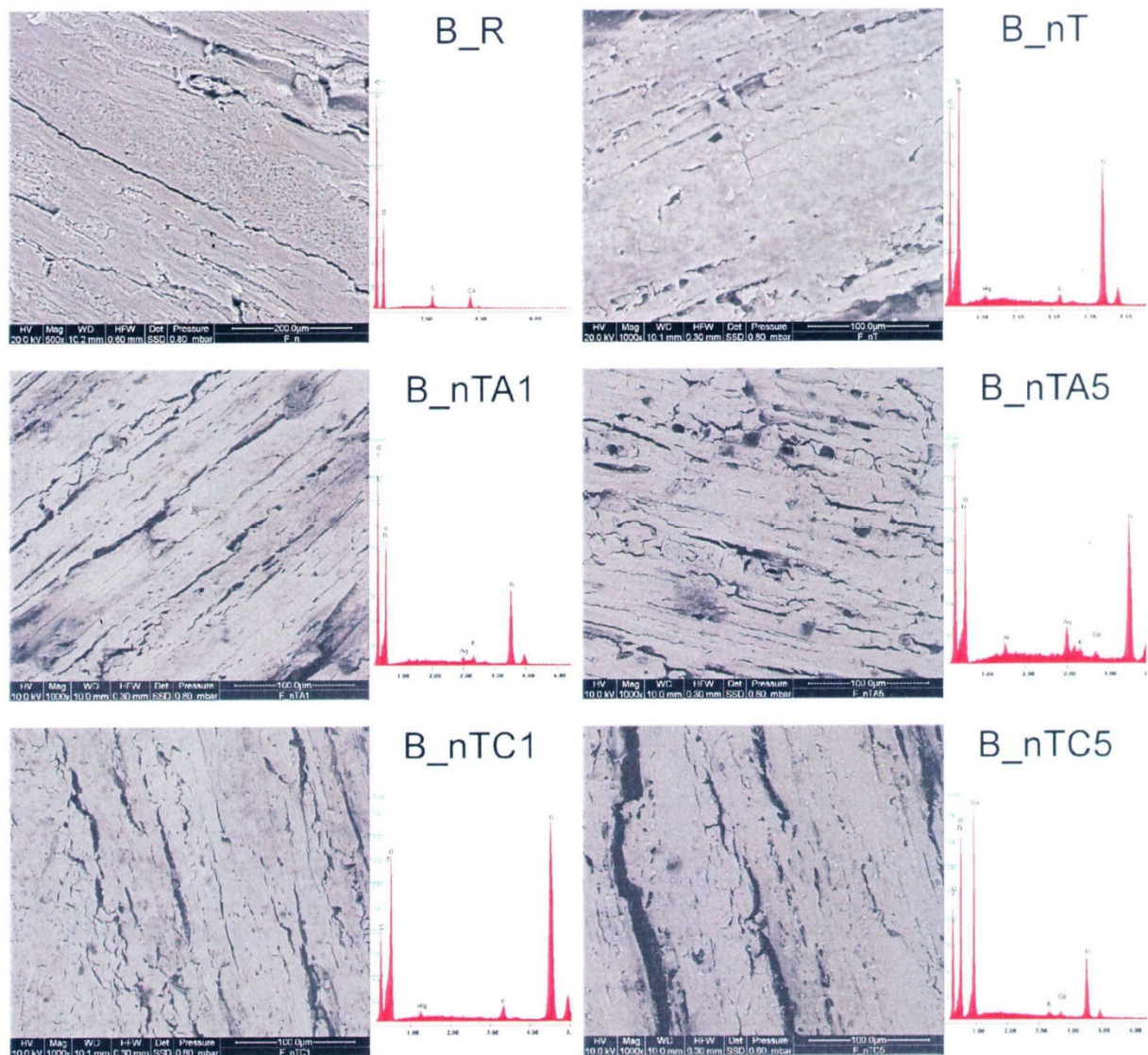


Fig. 3. Microscopic analyses of beech surfaces before mould test, untreated and treated: SEM images (magnitude 500 $\times$  for untreated wood, 1.000 $\times$  for treated surfaces) and EDS spectra (to the right of the corresponding SEM images)

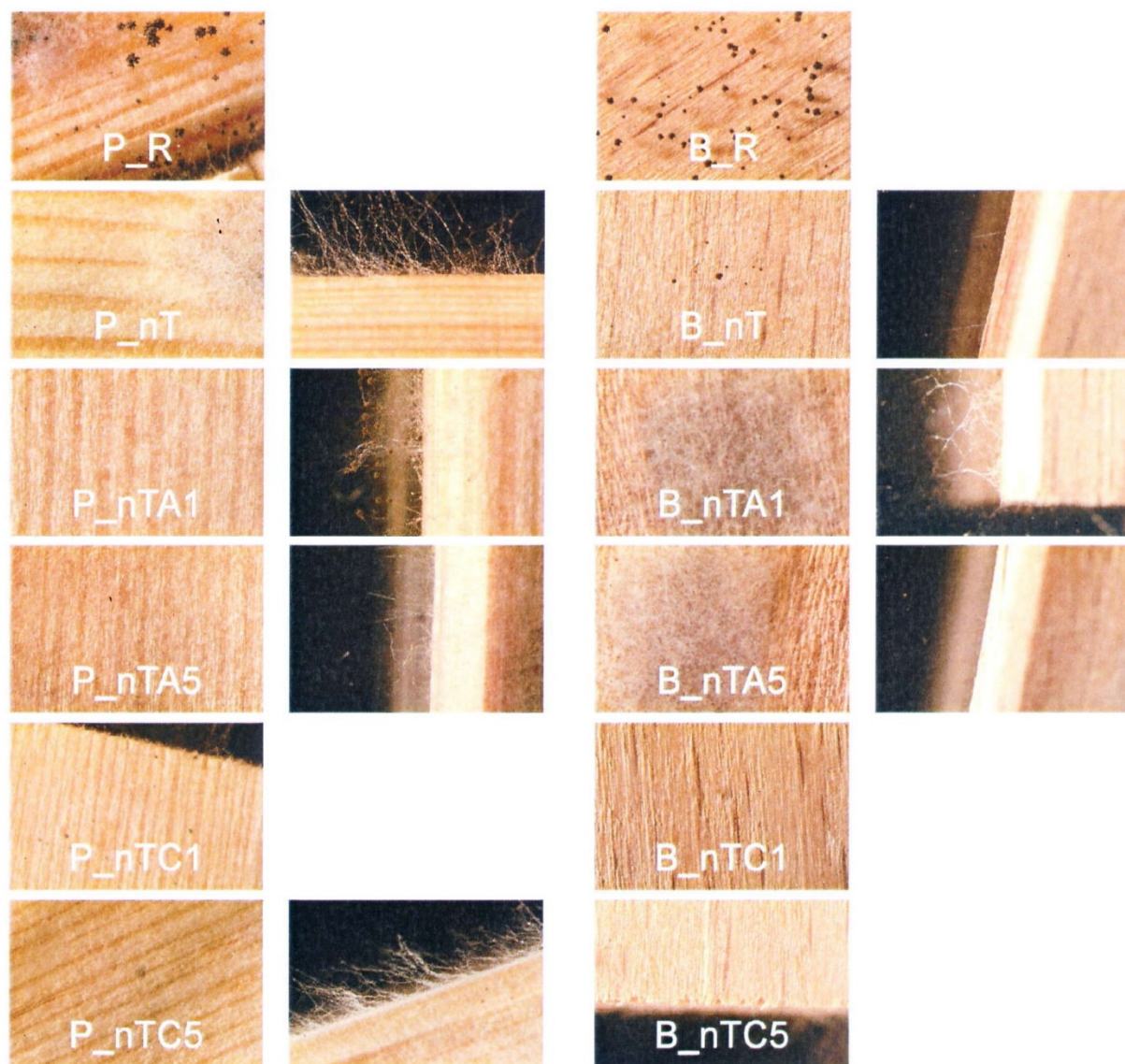


Fig. 4. Wood surfaces observed by stereomicroscope after two weeks of mould test: pine (left columns) and beech (right columns). Top surfaces and occasionally lateral borders (to the right of the corresponding top surface) are presented. The presence of wide and thick white mycelium in some top surfaces (P\_R, P\_nT, B\_nTA1, B\_nTA5) identifies the inoculation area on which *A. niger* could develop with limited inhibition by nanotreatments



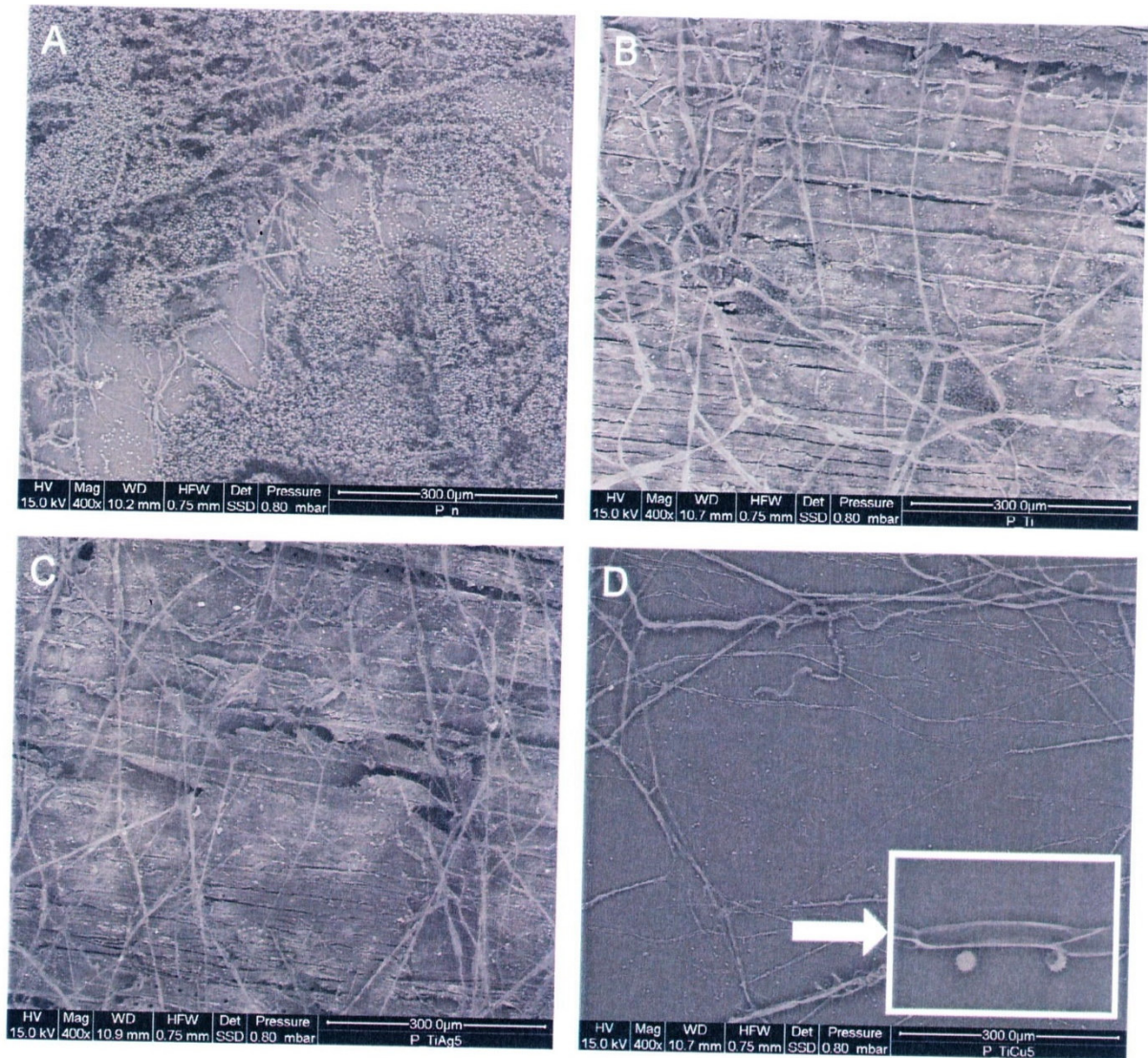


Fig. 5. SEM images of *A. niger* development on pine surfaces (magnitude 400×).  
A. Untreated surface. B. nT. C. nTAg5. C. nTCu5; (arrow) emptied hyphae



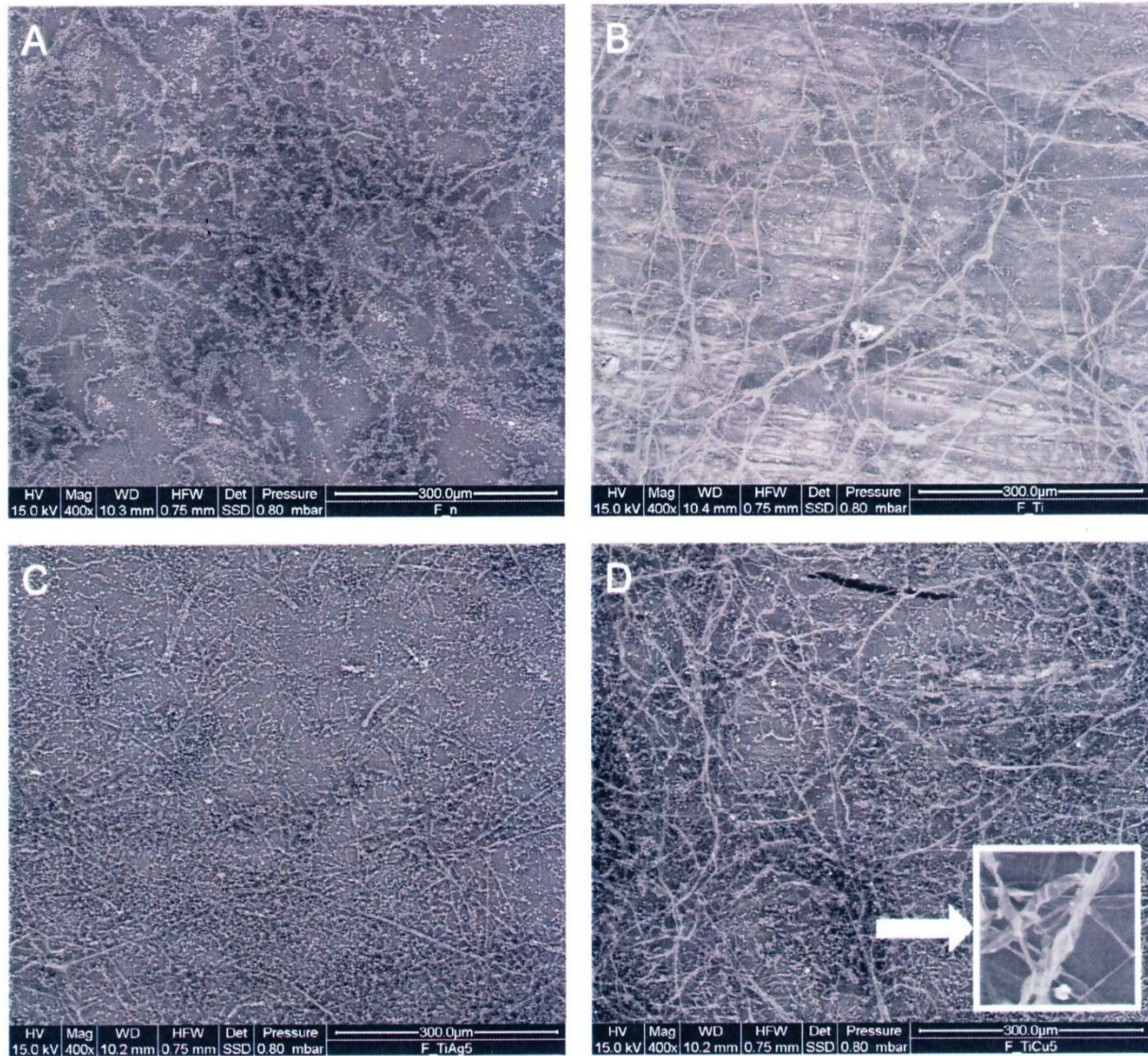


Fig. 6. SEM images of *A. niger* development on beech surfaces (magnitude 400×). A. Untreated surface. B. nT. C. nTA5. D. nTCu5; (arrow) emptied hyphae

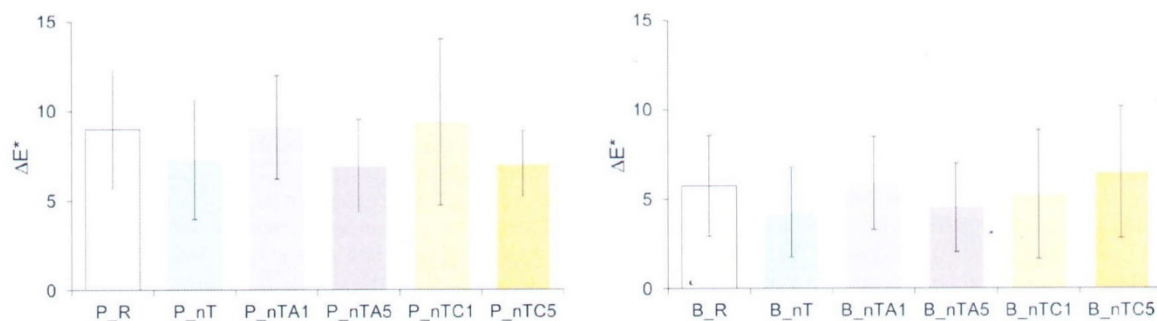


Fig. 7. Colour changes ( $\pm$  standard deviations) due to mould growth after 4 weeks ( $n = 10$ ), pine (left) and beech (right) specimens

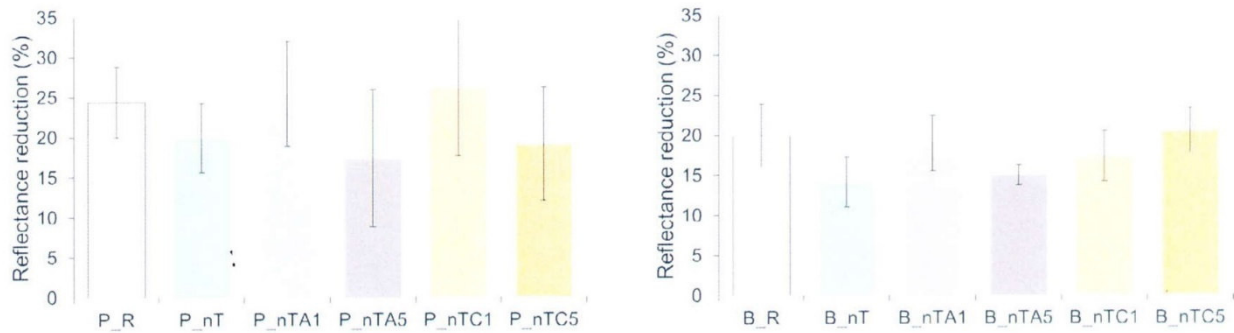


Fig. 8. Average reflectance reduction ( $\pm$ standard deviations) due to mould growth after 4 weeks ( $n = 10$ ), pine (left) and beech (right) specimens.

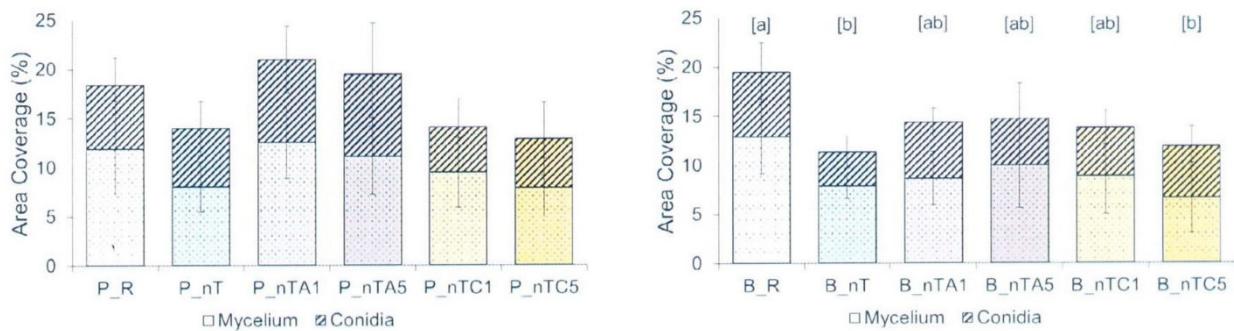


Fig. 8. Average reflectance reduction ( $\pm$ standard deviations) due to mould growth after 4 weeks ( $n = 10$ ), pine (left) and beech (right) specimens

Table 1

Nanoproducts tested, designations – samples identified by a wood id-letter, nanotreatment acronym and a number standing for the percentage of metallic nanoadditives used in the sol composition – and amount of sol applied on wood (average values  $\pm$  standard deviation,  $n = 10$ ).

Nanoparticles	Composition	Pine		Beech	
		Designation	Average sol amount (g/m <sup>2</sup> )	Designation	Average sol amount (g/m <sup>2</sup> )
–	Untreated reference	P_R	–	B_R	–
Titanium dioxide	TiO <sub>2</sub> (1 wt%)	P_nT	101 $\pm$ 24	B_nT	136 $\pm$ 20
Titanium dioxide, Silver	TiO <sub>2</sub> (1 wt%), Ag (1 mol%)	P_nTA1	110 $\pm$ 14	B_nTA1	131 $\pm$ 16
Titanium dioxide, Silver	TiO <sub>2</sub> (1 wt%), Ag (5 mol%)	P_nTA5	92 $\pm$ 15	B_nTA5	106 $\pm$ 13
Titanium dioxide, Copper	TiO <sub>2</sub> (1 wt%), Cu (1 wt%)	P_nTC1	114 $\pm$ 14	B_nTC1	111 $\pm$ 12
Titanium dioxide, Copper	TiO <sub>2</sub> (1 wt%), Cu (5 wt%)	P_nTC5	87 $\pm$ 16	B_nTC5	89 $\pm$ 5

Table 2

Colour changes ( $\pm$ standard deviations) after treatment ( $n = 10$ ).

	Before treatment			After treatment			
	L*	a*	b*	L*	a*	b*	$\Delta E^*$
<i>Pine</i>							
P_R	83.05	4.50	23.84	–	–	–	–
P_nT	83.31	4.43	23.70	83.24	5.08	23.86	1.19 $\pm$ 0.84
P_nTA1	82.98	4.59	23.98	77.55	5.22	20.28	6.64 $\pm$ 1.66
P_nTA5	82.70	4.59	24.09	76.25	7.70	21.81	7.53 $\pm$ 2.00
P_nTC1	83.65	4.24	23.38	83.67	4.72	23.22	0.85 $\pm$ 0.39
P_nTC5	83.39	4.40	23.60	83.65	4.55	23.12	0.88 $\pm$ 0.60
<i>Beech</i>							
B_R	70.20	9.45	21.55	–	–	–	–
B_nT	68.77	9.83	21.82	70.04	9.28	21.16	1.63 $\pm$ 0.87
B_nTA1	70.57	9.43	22.06	69.48	9.29	19.93	2.72 $\pm$ 1.00
B_nTA5	69.30	9.80	21.67	67.82	9.75	20.68	1.98 $\pm$ 0.44
B_nTC1	68.97	9.83	21.96	70.00	9.47	21.49	1.46 $\pm$ 0.45
B_nTC5	68.45	9.69	21.89	69.79	9.06	21.06	1.73 $\pm$ 0.66